ARMY RESEARCH LABORATORY

X-ray Diffraction as a Means to Assess Fatigue Performance of Shot-Peened Materials

by Daniel J. Snoha and Scott M. Grendahl

ARL-TR-6039 **June 2012**

NOTICES

Disclaimers

The findings in this report are not to be construed as an official Department of the Army position unless so designated by other authorized documents.

Citation of manufacturer's or trade names does not constitute an official endorsement or approval of the use thereof.

Destroy this report when it is no longer needed. Do not return it to the originator.

Army Research Laboratory
Aberdeen Proving Ground, MD 21005-5069

ARL-TR-6039 **June 2012**

X-ray Diffraction as a Means to Assess Fatigue Performance of Shot-Peened Materials

Daniel J. Snoha and Scott M. Grendahl
Weapons and Materials Research Directorate, ARL

REPORT DOCUMENTATION PAGE	Form Approved OMB No. 0704-0188

1. REPORT DATE *(DD-MM-YYYY)*	2. REPORT TYPE	3. DATES COVERED (From - To)
June 2012	Final	September 2005–April 2009

4. TITLE AND SUBTITLE
X-ray Diffraction as a Means to Assess Fatigue Performance of Shot-Peened Materials

5a. CONTRACT NUMBER

5b. GRANT NUMBER

5c. PROGRAM ELEMENT NUMBER

6. AUTHOR(S)
Daniel J. Snoha and Scott M. Grendahl

5d. PROJECT NUMBER
589D31589U3

5e. TASK NUMBER

5f. WORK UNIT NUMBER

7. PERFORMING ORGANIZATION NAME(S) AND ADDRESS(ES)
U.S. Army Research Laboratory
ATTN: RDRL-WMM-F
Aberdeen Proving Ground, MD 21005-5069

8. PERFORMING ORGANIZATION REPORT NUMBER
ARL-TR-6039

9. SPONSORING/MONITORING AGENCY NAME(S) AND ADDRESS(ES)
U.S. Army Aviation and Missile Research, Development, and Engineering Center
Redstone Arsenal, AL 35898

10. SPONSOR/MONITOR'S ACRONYM(S)
AMRDEC

11. SPONSOR/MONITOR'S REPORT NUMBER(S)

12. DISTRIBUTION/AVAILABILITY STATEMENT
Approved for public release; distribution is unlimited.

13. SUPPLEMENTARY NOTES

14. ABSTRACT
Residual compressive stresses can contribute significantly to the enhancement of fatigue performance. Conventional shot peening is a process for imparting beneficial stresses at the surface and into the near-surface region of a metal component. X-ray diffraction provides a method to nondestructively characterize residual stress by the direct measurement of elastic strain in the microscopic structure. Plastic strain can be evaluated by the width of the diffraction peak. This report presents elastic and plastic strain data from residual stress measurements performed on four aviation materials shot peened to various Almen A-scale intensities by two different vendors. Fatigue performance in terms of endurance limit was determined using unnotched, round $K_t = 1$ test specimens. In general, the deepest levels of compression were associated with higher shot-peening intensities. However, the best fatigue performance and highest surface residual compressive stresses were observed on the lower end of the peening intensity range.

15. SUBJECT TERMS
x-ray diffraction, residual stress, elastic strain, peak width, plastic strain, fatigue performance, shot peen, Almen intensity

16. SECURITY CLASSIFICATION OF:			17. LIMITATION OF ABSTRACT	18. NUMBER OF PAGES	19a. NAME OF RESPONSIBLE PERSON
a. REPORT	b. ABSTRACT	c. THIS PAGE			Daniel J. Snoha
Unclassified	Unclassified	Unclassified	UU	28	19b. TELEPHONE NUMBER (*Include area code*) 410-306-0821

Standard Form 298 (Rev. 8/98)
Prescribed by ANSI Std. Z39.18

Contents

List of Figures

List of Tables

Acknowledgments

The authors acknowledge the U.S. Army Aviation and Missile Command, Redstone Arsenal, AL, for funding this work. We also acknowledge Mr. Benjamin Hardisky from the Aberdeen Test Center, Aberdeen Proving Ground, MD, for electropolishing the disk specimens. Finally, we thank Ms. Beth Matlock, Technology for Energy Corporation, Knoxville, TN, for assisting in the analysis of the residual stress data.

INTENTIONALLY LEFT BLANK.

1. Introduction

It is widely accepted that residual compressive stresses in aviation materials enhance fatigue performance. Conventional shot peening is a process for imparting beneficial residual compressive stresses at the surface and into the near-surface region of a component (*1–4*). The magnitude of the induced stresses is primarily a function of the ultimate tensile strength of the material being peened, while the depth of the cold-worked layer is related to peening parameters such as media (shot) size, intensity, and coverage.

Shot peening is performed during both manufacturing and maintenance overhaul of flight critical components on U.S. Army aviation platforms. The inherent variables associated with the process provide a wide range of performance in terms of fatigue resistance and the magnitude and depth of the induced residual compressive stresses. However, without a costly component-based fatigue assessment for each combination of shot-peening variables, assigning flight risk due to possible improper processing is difficult. A thorough understanding of fatigue performance evaluated against the gamut of variables provides information with which to prescribe risk for each material system and associated shot-peening condition.

Residual stresses are stresses that remain in a material after all external loading has been removed. These stresses are elastic and develop (or change) as a consequence of mechanical working processes (such as shot peening), phase transformation, thermal expansion, etc. X-ray diffraction (XRD) can be used to nondestructively determine residual stress in polycrystalline materials by the direct measurement of strain in the microscopic structure (*5*, *6*). Elastic strain is characterized by a shift in the peak position of the diffraction pattern, and plastic strain can be evaluated by the width of the diffraction peak, usually at half maximum intensity (*7*). XRD techniques also have been employed to study the mechanical behavior of materials, with particular emphasis on the detection of fatigue damage and the effect that residual stress has on the retardation of crack growth (*8*). Coupling x-ray elastic strain and plastic strain data provides a means to better assess the effectiveness of the shot-peening process as it relates to fatigue performance.

2. Experimental Procedure

Four materials that represent those most commonly utilized for U.S. Army aviation shot-peened components were selected for this investigation. Table 1 lists the materials along with the production specification and supplier-tested ultimate tensile strength data. Bar stock was machined into disk and fatigue specimens for residual stress analysis and fatigue testing.

Table 1. Aviation materials investigated.

Material	Specification	Ultimate Tensile Strength (MPa [ksi])
4340 steel	AISI/SAE E4340 (*9*)	1117.0 (162.0)
Carburized 9310 steel	AMS 2759/1C (*10*)	1303.2 (189.0)
Beta-STOA titanium 6Al-4V	AMS 4928Q (*11*)	1027.4 (153.0)
Aluminum 7075-T73	AMS-QQ-A 225/9 (*12*)	535.1 (77.6)

Note: Beta-STOA = beta-solution treated and overaged.

2.1 Shot-Peening Intensity

The U.S. Army Research Laboratory, in conjunction with the U.S. Army Aviation and Missile Research Development and Engineering Center, prescribed the shot-peening intensity range relevant to each aviation material examined. Two different vendors, heretofore referred to as V1 and V2, established the processing parameters necessary to achieve the desired peening intensities. Since many combinations of media (shot) size, air pressure, nozzle size, nozzle (impingement) angle, nozzle distance (standoff), and flow rate can be used to achieve the same Almen intensity, the exact parameters utilized are presented in table 2.

Intensity is normally specified at the 100% coverage level, while 200% coverage is the typical callout for aviation materials to add a factor of safety for flight critical components. Under the same processing parameters, intensity increases with coverage until saturation is achieved. Both the 100% and 200% coverage actual intensity levels are given in table 2.

For this work, the nozzle size was maintained at 6.35 mm (0.25 in). Steel shot with a hardness range of 45–52 HRC was used to peen the Almen strips. Coverage was verified via visual inspection as a minimum of 100%. The disk and fatigue specimens studied were subsequently shot peened at the 200% coverage level to the specific intensities established for each material: 4A, 8A, and 12A for steel; 4A, 8A, 11.5A, and 12A for titanium; and 4A, 10A, 12A, and 14A for aluminum. Three disk specimens were shot peened to the specified intensities by both vendors using shot sizes of S110, S170, and S230 for the steel, titanium, and aluminum, respectively.

2.2 Residual Stress Analysis

X-ray diffraction residual stress measurements were made on the shot-peened disk and fatigue test specimens using a Technology for Energy Corporation model 1610 X-Ray Stress Analysis System employing the $\sin^2\psi$ (multiple exposure) stress-measuring technique. The XRD collection parameters are listed in table 3. The x-ray elastic constants required to calculate the macroscopic residual stress from the measured elastic strain agreed with common practice. Residual stress measurements were performed on the disk specimens at the center and at a radial outward (edge) location. The orientation of the edge location was chosen arbitrarily. All disk specimens were 9.5 mm (0.375 in) thick. The diameter of the steel disks was 25.4 mm, (1.0 in)

and the titanium and aluminum specimens were 19.1 mm (0.75 in) in diameter. The unnotched, round fatigue test specimens were measured at the center of the gage section in three equally spaced circumferential locations, with the 0° orientation being chosen arbitrarily.

Table 2. Shot peen processing parameters and resultant Almen A-scale intensities.

Material	Shot Peening Vendor	Specified Almen Intensity	Shot Size	Air Pressure (psi)	Nozzle Angle (degrees)	Nozzle Distance (in)	Flow Rate (lb/min)	Resultant Almen Intensity at 100% Coverage	Resultant Almen Intensity at 200% Coverage
4340 and 9310 steel	V1	4A ± 0.5	S110	15–20	65	7	9.0	0.0039	0.0042
—	V2	4A ± 0.5	—	10	90	8	2.6	0.0040	0.0044
—	V1	8A ± 0.5	—	60–65	65	9	8.5	0.0076	0.0081
—	V2	8A ± 0.5	—	33	90	8	10.2	0.0079	0.0084
—	V2	12A ± 0.5	—	58	90	8	5.3	0.0121	0.0130
Titanium 6Al-4V	V1	4A ± 0.5	—	20	65	11	9.2	0.0040	0.0043
—	V1	8A ± 0.5	—	40–45	65	9	8.8	0.0080	0.0083
—	V1	11.5A-0.0 ± 0.5	—	65–75	90	7	7.4	0.0115	0.0119
—	V2	12A ± 0.5	—	60	90	3	4.5	0.0122	0.0130
Aluminum 7075	V1	4A ± 0.5	S230	10	65	11	10.1	0.0040	0.0044
—	V1	10A ± 0.5	—	40	65	7	10.1	0.0103	0.0107
—	V2	10A ± 0.5	—	30	90	8	16	0.0100	0.0110
—	V1	12A ± 0.5	—	55	65	7	10.1	0.0120	0.0124
—	V2	12A ± 0.5	—	35	90	8	16	0.0122	0.0131
—	V1	14A-0.0 ± 0.5	—	70	65	7	10.1	0.0140	0.0145

Table 3. X-ray diffraction residual stress measurement parameters.

Material	Radiation	Lattice Planes	Specimen Type	Irradiated Area Size/Shape
4340 and 9310 steel	CrKα	(211)	Disk	3 mm/round
—	—	—	Fatigue	1.5 × 5 mm/rectangular
Titanium 6Al-4V	CuKα	(213)	Disk	2 mm/round
—	—	—	Fatigue	1.5 × 5 mm/rectangular
Aluminum 7075	CuKα	(333,511)	Disk	2 mm/round
—	—	—	Fatigue	1.5 × 5 mm/rectangular

Residual stresses were measured only at the surface on the fatigue specimens, whereas the disks were measured at the surface and at the 0-, 0.03-, 0.05-, 0.13-, 0.18-, and 0.25-mm (0-, 1-, 2-, 5-, 7-, and 10-mil) depths. The subsurface stress profiles were characterized on the disks by alternately performing XRD measurements then electropolishing away layers of material.

2.3 Electropolishing

A Struers Lectropol-5 electropolisher was utilized to remove material from the shot-peened disk specimens. Two electrolytes were used for the chemical polishing operations. The steel and titanium electrolyte contained 6% perchloric acid, 35% butyl cellusolve, and 59% methanol. The electrolyte for the aluminum was comprised of 6.3% perchloric acid, 13.7% water, 10% butyl cellusolve, and 70% ethanol. A linear height gage with a vernier was used for measuring the depth to which the disks were polished at the center and edge locations. Both measurements were necessary because of the tendency of the center and edge removal rates to vary. Additionally, multiple cycles of polishing and measuring were employed to reach a required depth.

2.4 Fatigue Testing

Fatigue strength was tested using unnotched, round $K_t = 1$ specimens (shown in figure 1) on 45 tf (100 kip) Instron and MTS Systems Corp. test frames, with sinusoidal oscillation at a frequency of 20 Hz and an R-ratio of 0.1. A Nicolet model 4094C oscilloscope was utilized to optimize the conditions of the sinusoidal wave and loop-shaping parameters of the closed loop feedback systems on the test frame. All tests were conducted in air at room temperature. The run-out stop point was 2 million cycles.

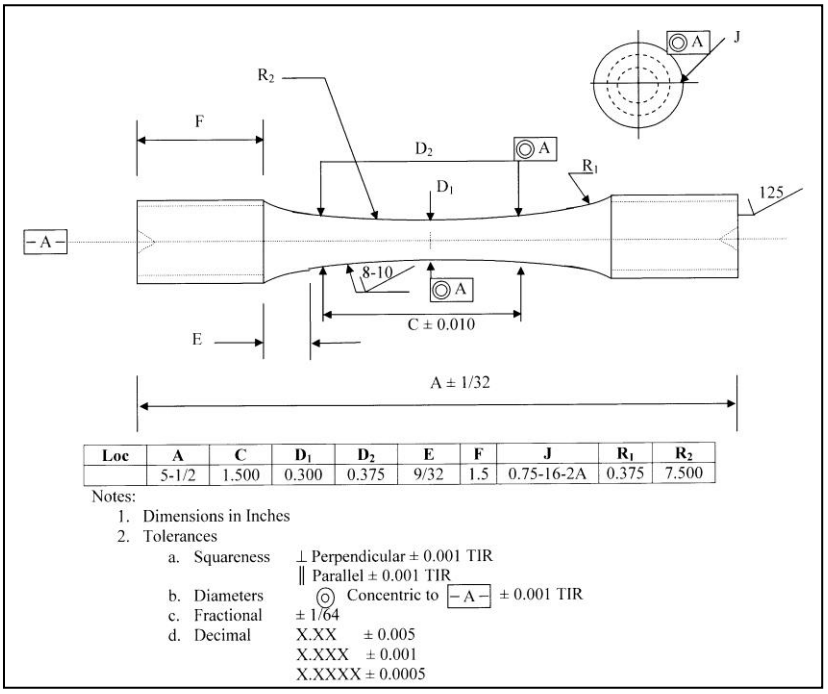

Loc	A	C	D_1	D_2	E	F	J	R_1	R_2
	5-1/2	1.500	0.300	0.375	9/32	1.5	0.75-16-2A	0.375	7.500

Notes:
1. Dimensions in Inches
2. Tolerances
   a. Squareness ⊥ Perpendicular ± 0.001 TIR; ∥ Parallel ± 0.001 TIR
   b. Diameters ◎ Concentric to -A- ± 0.001 TIR
   c. Fractional ± 1/64
   d. Decimal X.XX ± 0.005; X.XXX ± 0.001; X.XXXX ± 0.0005

Figure 1. Schematic of unnotched, round $K_t = 1$ fatigue test specimens.

3. Results

3.1 Residual Stress and Diffraction Peak Width Data

The results of x-ray diffraction residual stress analysis are presented in graphical form in figures 2–5. The individual datasets represent the average residual stress (RS) and diffraction peak full width-half maximum (FWHM) values from six separate measurements made on the shot-peened disk specimens. As previously reported (*13*), the residual stress distributions and magnitudes were approximately equivalent at the center and edge measurement locations for all materials tested. The observed (as-collected) surface RS data were corrected for stress relaxation caused by electropolishing material removal and for the differences in the depths of penetration of the x-ray beam at the different ψ angles. V1 and V2 represent the two different shot-peening vendors, while 4A, 8A, 10A, 11.5A, 12A, and 14A are the specified Almen A-scale intensities. Note that a negative sign (-) indicates a compressive stress.

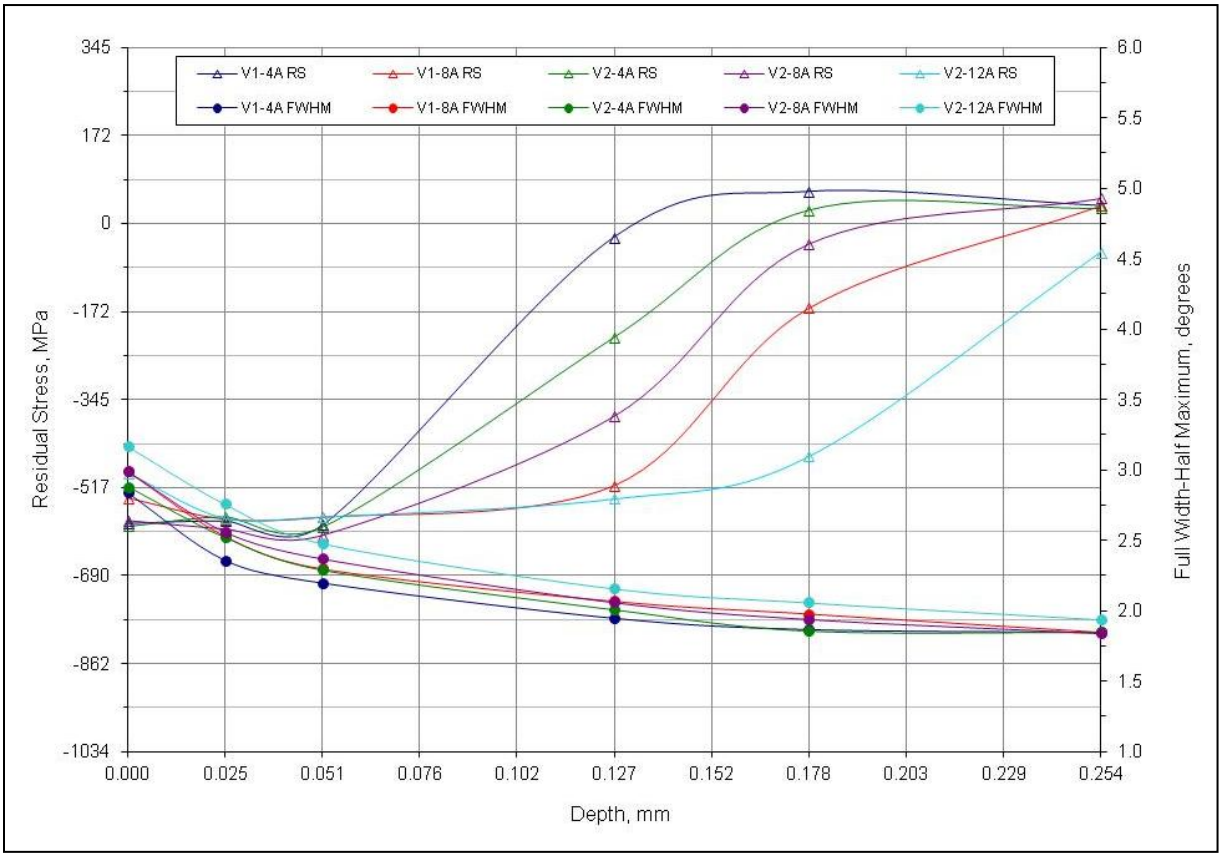

Figure 2. Residual stress and diffraction peak width data from the 4340 steel disks.

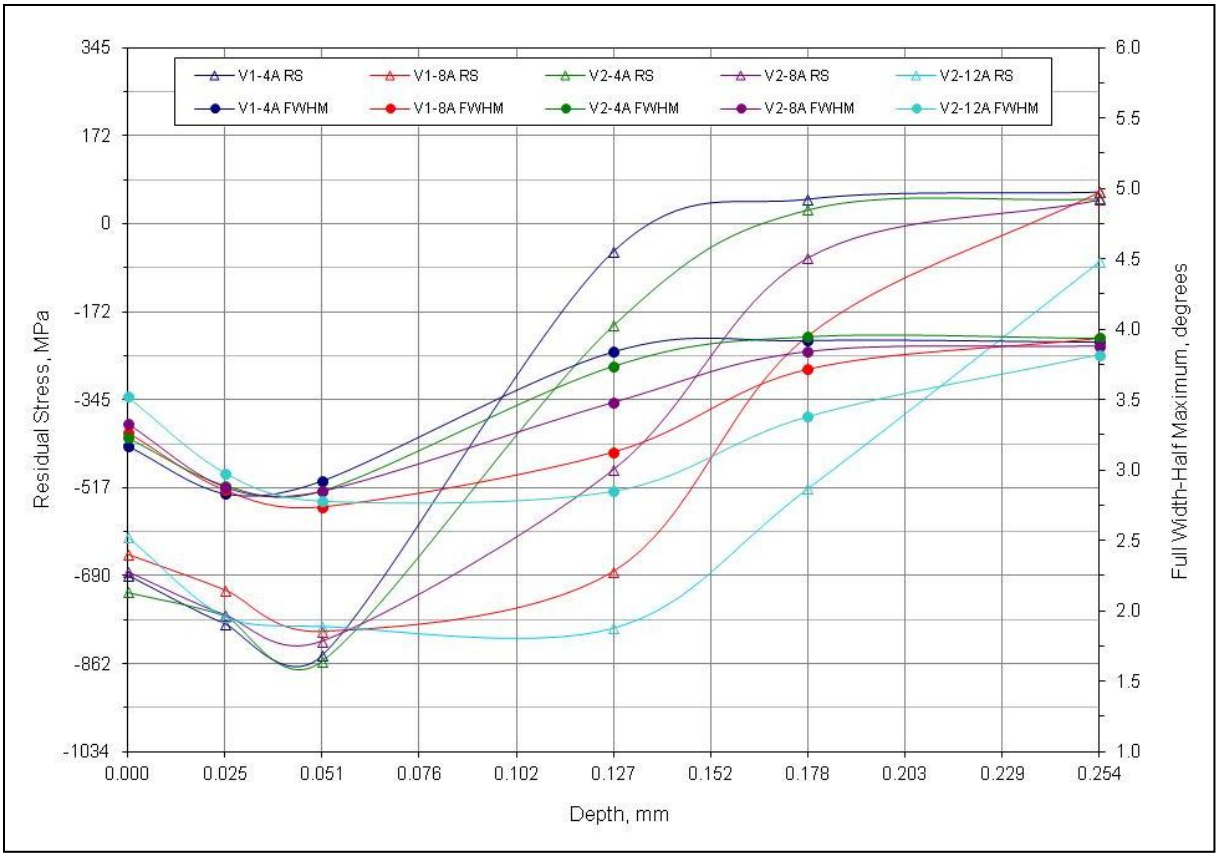

Figure 3. Residual stress and diffraction peak width data from the carburized 9310 steel disks.

3.1.1 The 4340 Steel

Surface residual stresses ranged from –593 MPa (–86.0 ksi) for V2-12A to –488 MPa (–70.8 ksi) for V1-4A. The maximum compressive stress for all intensities occurred between the 0.025 mm (0.001 in) and the 0.051 mm (0.002 in) measurement depths. Shot-peening intensity was observed to be directly related to depth of compression, with the residual stresses from the V2-12A disks remaining compressive through the deepest electropolished layer, 0.254 mm (0.010 in). The diffraction peak width trend lines were uniform for all intensities, with the largest values measured at the surface.

3.1.2 Carburized 9310 Steel

The residual stress and FWHM patterns were similar to those from the 4340 steel. However, due to the higher ultimate tensile strength of the carburized 9310 steel, the compressive stresses were greater in magnitude and extended deeper into the disks. The surface stresses averaged –671 ± 46 MPa (–97.3 ± 6.7 ksi), and the maximum compressive stress was measured at a nominal depth of the 0.051 mm (0.002 in). The diffraction peak width for all peening intensities was approximately uniform except at the 0.127-mm (5-mil) and 0.178-mm (7-mil) depths, where the spread in these values was 1.0° and 0.6°, respectively. In contrast to the 4310 steel, the largest peak widths were not found at the surface but rather at the deepest layer. This can likely be

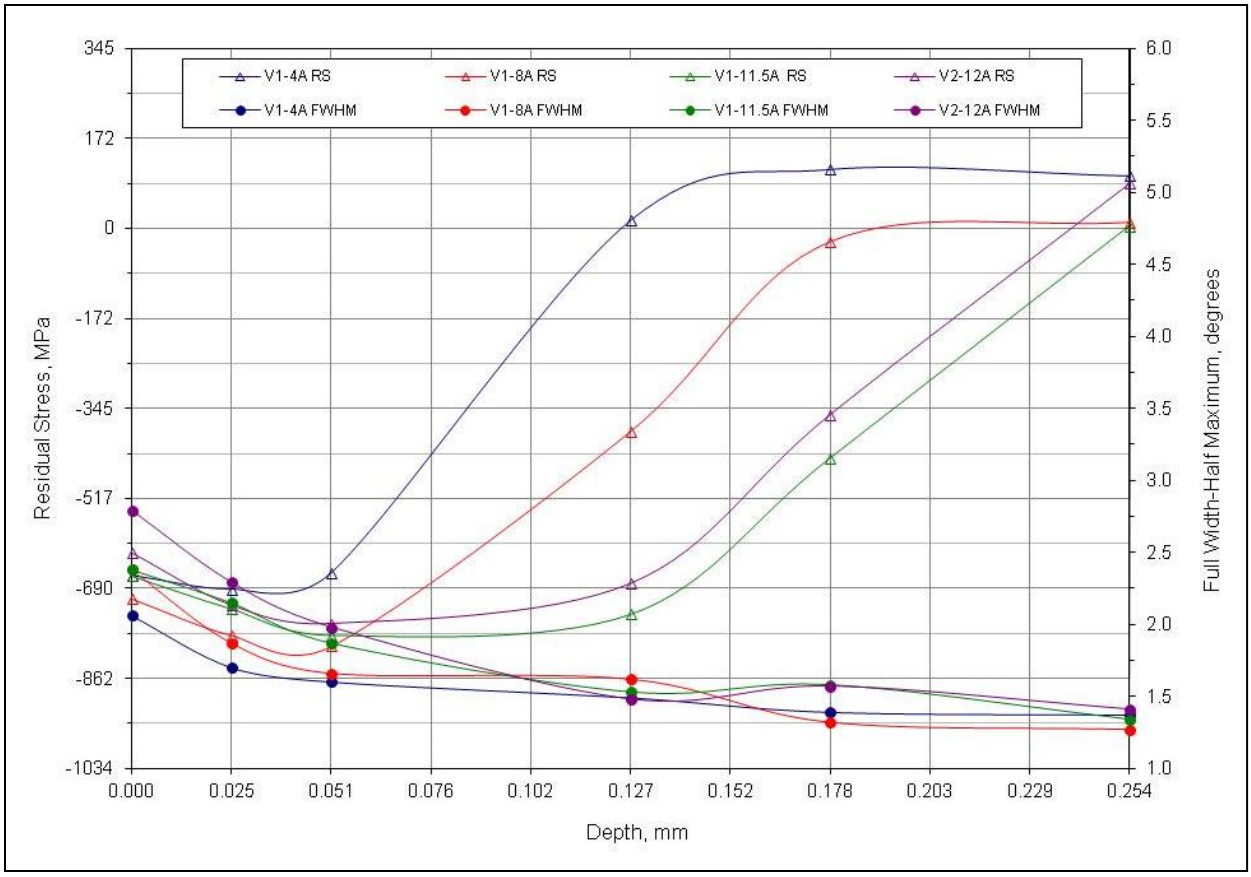

Figure 4. Residual stress and diffraction peak width data from the beta-STOA titanium 6Al-4V disks.

attributed to the hardness of the carburized surface limiting the amount of peening-induced plastic deformation relative to the bulk material. This observation has been reported elsewhere (*14*).

3.1.3 Aluminum 7075-T73

Only compressive residual stresses were measured at the surface and at all surface layers on the aluminum disks. The stress distributions were uniform and approximately equivalent in magnitude except for the V1-4A intensity, which produced the highest compressive stresses at the surface and the at 0.051-mm (1-mil) depth. However, at that depth, the 4A stress profile, unlike those from the 10A, 12A, and 14A intensities, trended linearly in a tensive direction to an almost zero stress condition at the deepest electropolished layer, 0.254 mm (0.010 in). The narrowest FWHM values also were associated with the V1-4A intensity, though the trend was similar to the other intensities. It was probable that while the 4A intensity was optimum for maximizing surface residual stress, it was deficient in pushing those stresses deep into the material. The maximum compressive stresses on the 10A, 12A, and 14A intensity specimens occurred between the 0.127 and 0.178 mm (0.005 and 0.007 in) electropolished layers.

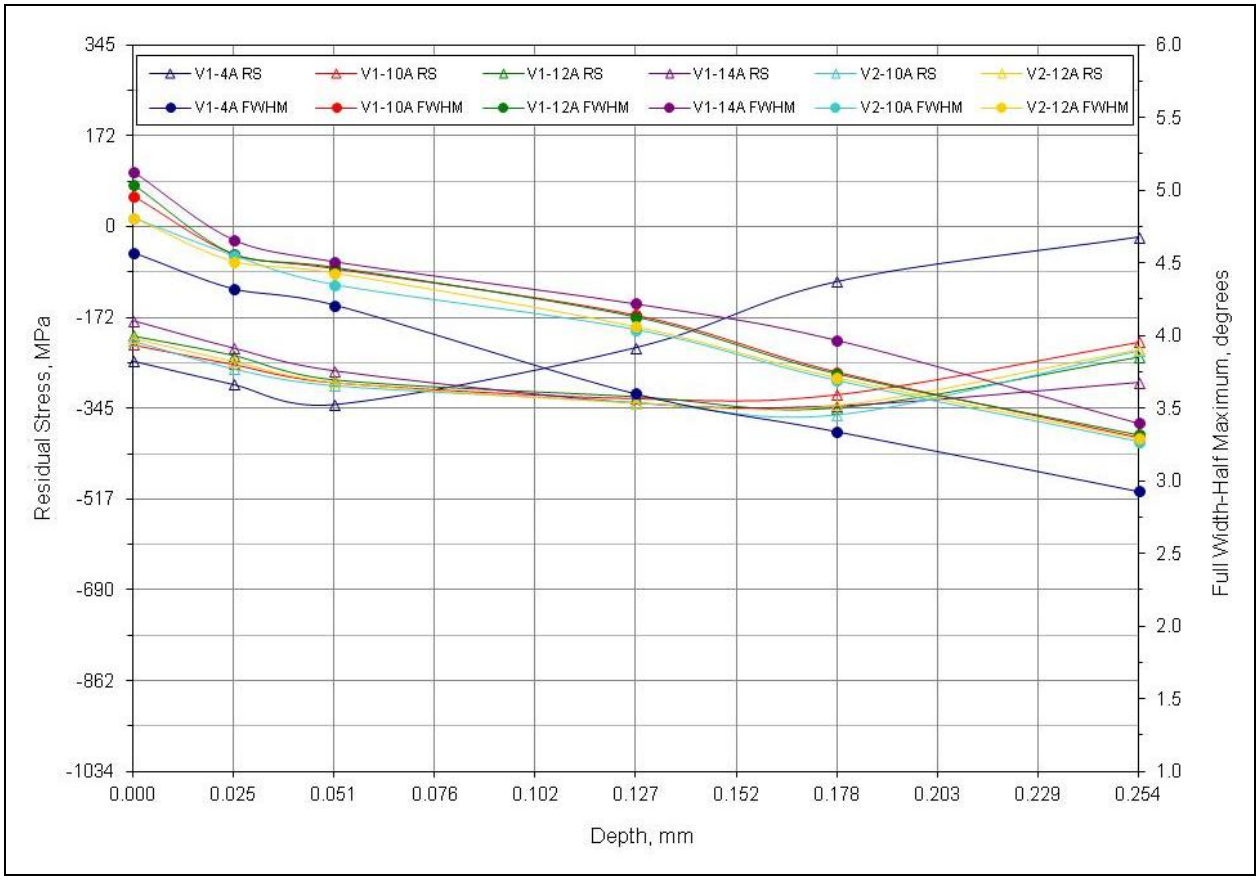

Figure 5. Residual stress and diffraction peak width data from the aluminum 7075-T73 disks.

3.1.4 Beta-STOA Titanium 6Al-4V

Approximately equivalent residual compressive stresses averaging 665 ± 51 MPa (96.5 ± 7.4 ksi) were measured at the surface of the titanium disks. As with the steel specimens that were shot peened to similar intensities, the maximum compressive stresses were found at or between the 0.025 mm (0.001 in) and the 0.051 mm (0.002 in) measurement depths. The V1-11.5A and V2-12A residual stress patterns were nearly identical, with the latter being predictably a little more compressive and extending deeper into the material. The largest diffraction peak widths were recorded at the surface, though the data varied by almost 0.75°, the biggest range of any of the four materials.

3.2 Fatigue Performance

The plotted data of cycles to failure vs. maximum stress are shown in figures 6–9. These data represent approximately 10 unnotched, round axial fatigue specimens (see figure 1) shot peened to the specified intensities at 200% coverage, compared with an identical unpeened baseline group. V1 and V2 represent the two different shot-peening vendors, while 4A, 8A, 10A, 11.5A, 12A, and 14A are the specified Almen A-scale intensities.

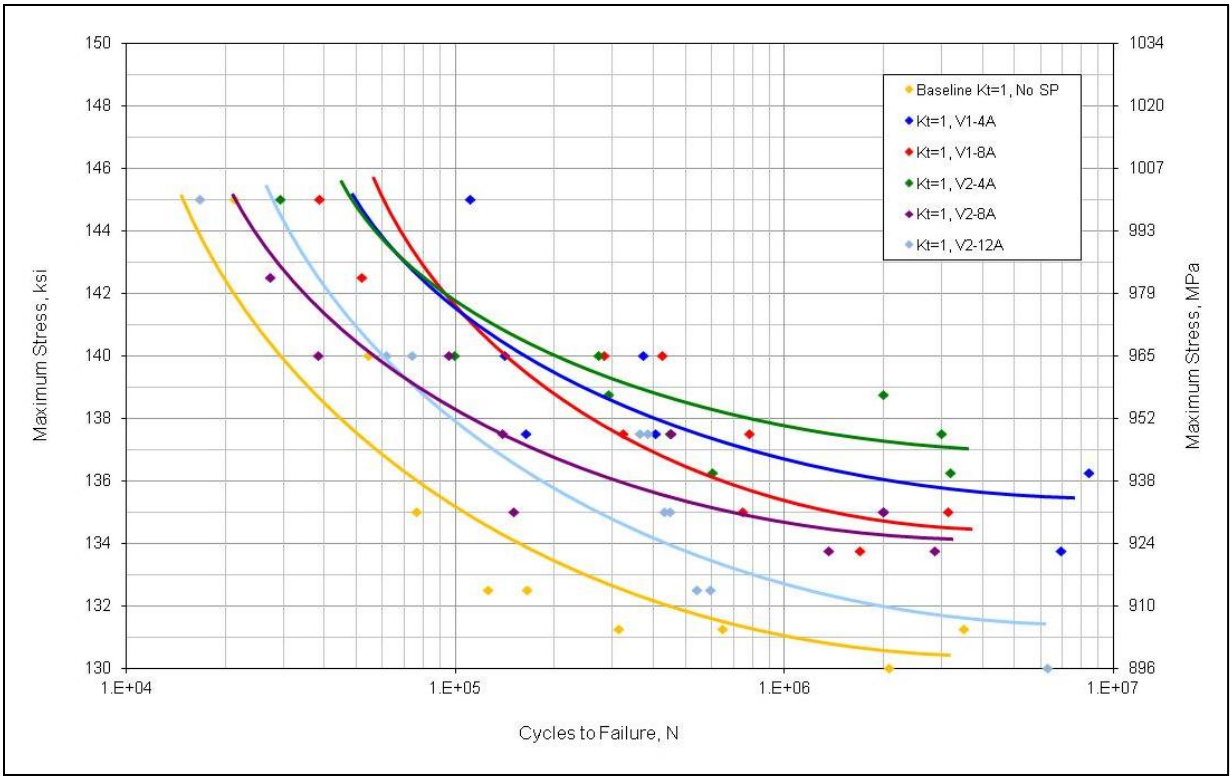

Figure 6. Fatigue data from the 4340 steel.

3.2.1 The 4340 Steel

The 4340 steel data demonstrated that the shot peening was beneficial in all cases. The 4A intensity from both vendors had the best performance in terms of endurance limit, and the 12A had the poorest, though all intensities showed an improvement over the baseline. There was clearly an inverse relationship between shot-peening intensity and fatigue performance.

3.2.2 Carburized 9310 Steel

The profiles from the carburized 9310 steel were comparable in trend to the 4340 steel. Again, the V1- and V2-4A shot-peening intensities provided the best fatigue performance, while the 12A had the poorest. However, with this material, the 12A and the V1-8A intensity performed worse than the baseline. (There was no accounting for the variation in the V1- and V2-8A fatigue results other than perhaps a difference in vendor processing.) The inverse relation between intensity and fatigue performance was still prevalent.

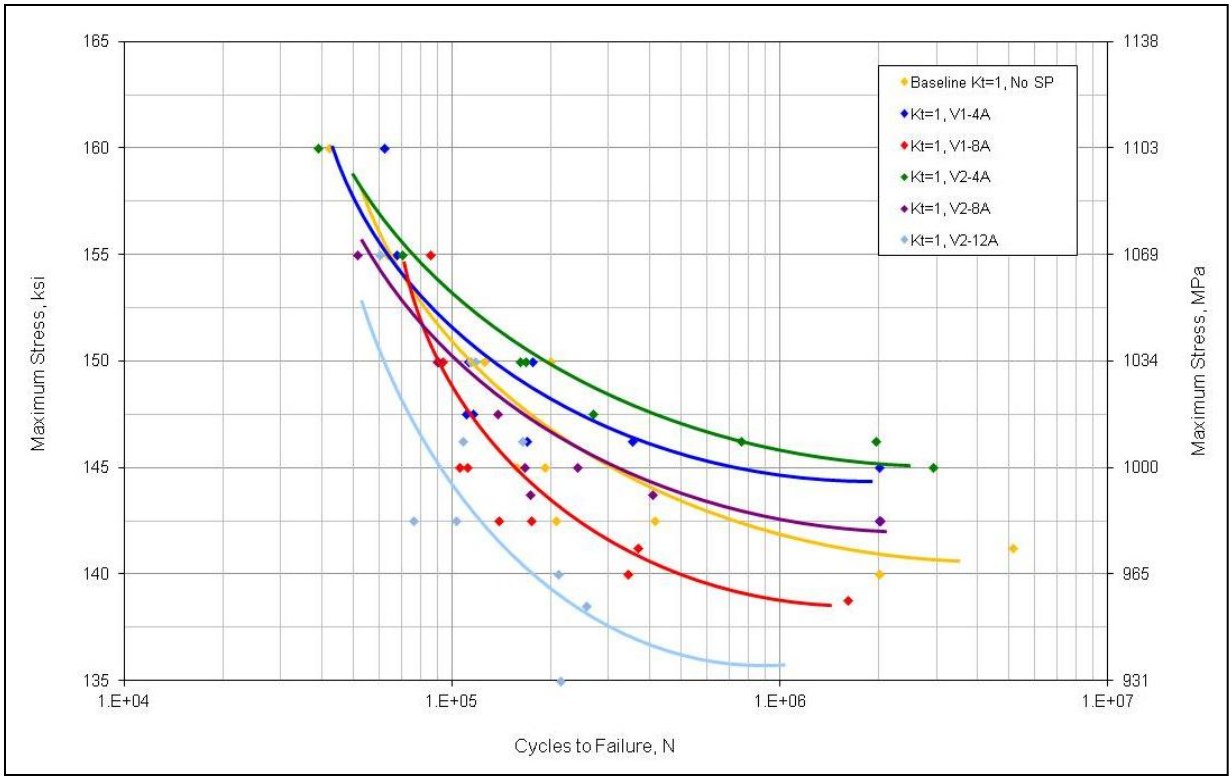

Figure 7. Fatigue data from the carburized 9310 steel.

3.2.3 Beta-STOA Titanium 6Al-4V

The titanium 6-4 fatigue data exhibited similar trends to the 9310 steel material. Low shot-peening intensities (4A and 8A) improved fatigue performance over the baseline specimens, while higher intensities (11.5A and 12A) proved detrimental. Uniformly, an inverse relationship of intensity and fatigue was observed.

3.2.4 Aluminum 7075-T73

Unlike the other three aviation materials investigated, the aluminum 7075 demonstrated that shot peening, under the specified intensities, was not beneficial to fatigue performance. Only the lightest intensity specimens, 4A, approximated the results from the unpeened baseline group. This material, however, did follow the previously noted inverse relationship between peening intensity and fatigue performance.

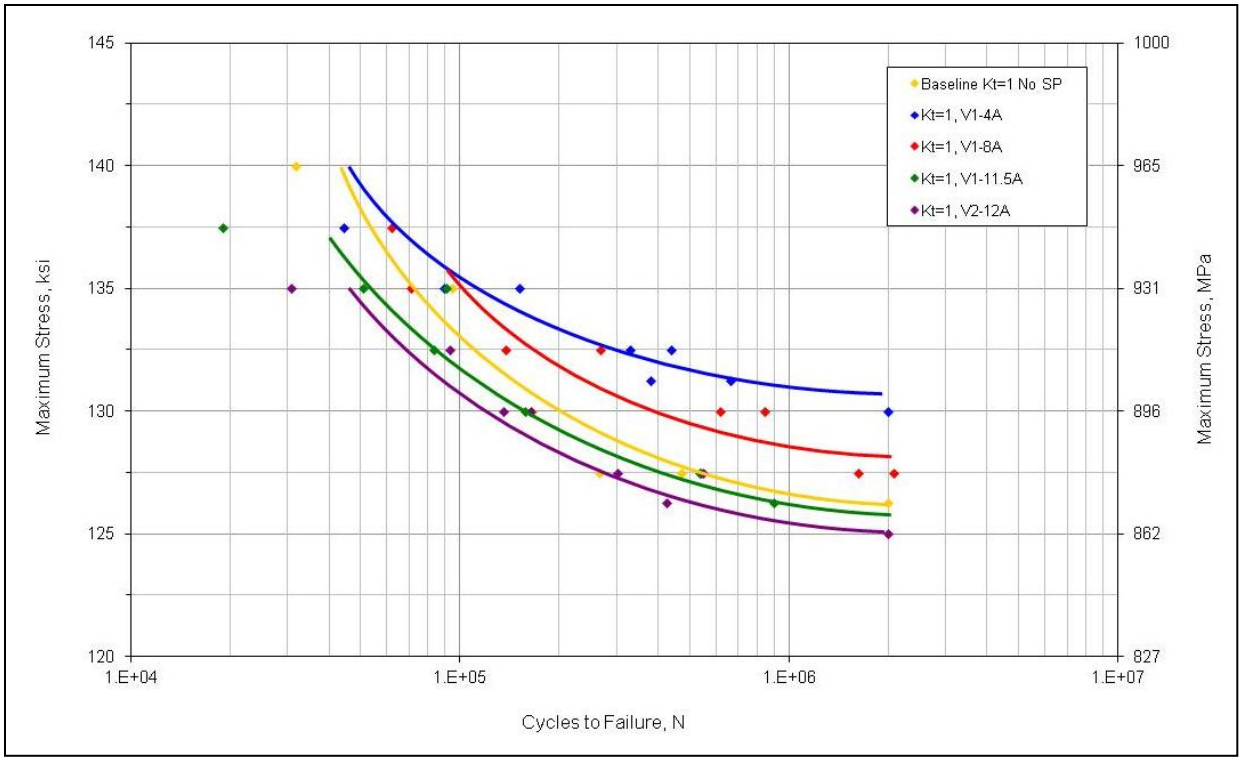

Figure 8. Fatigue data from the beta-STOA titanium 6Al-4V.

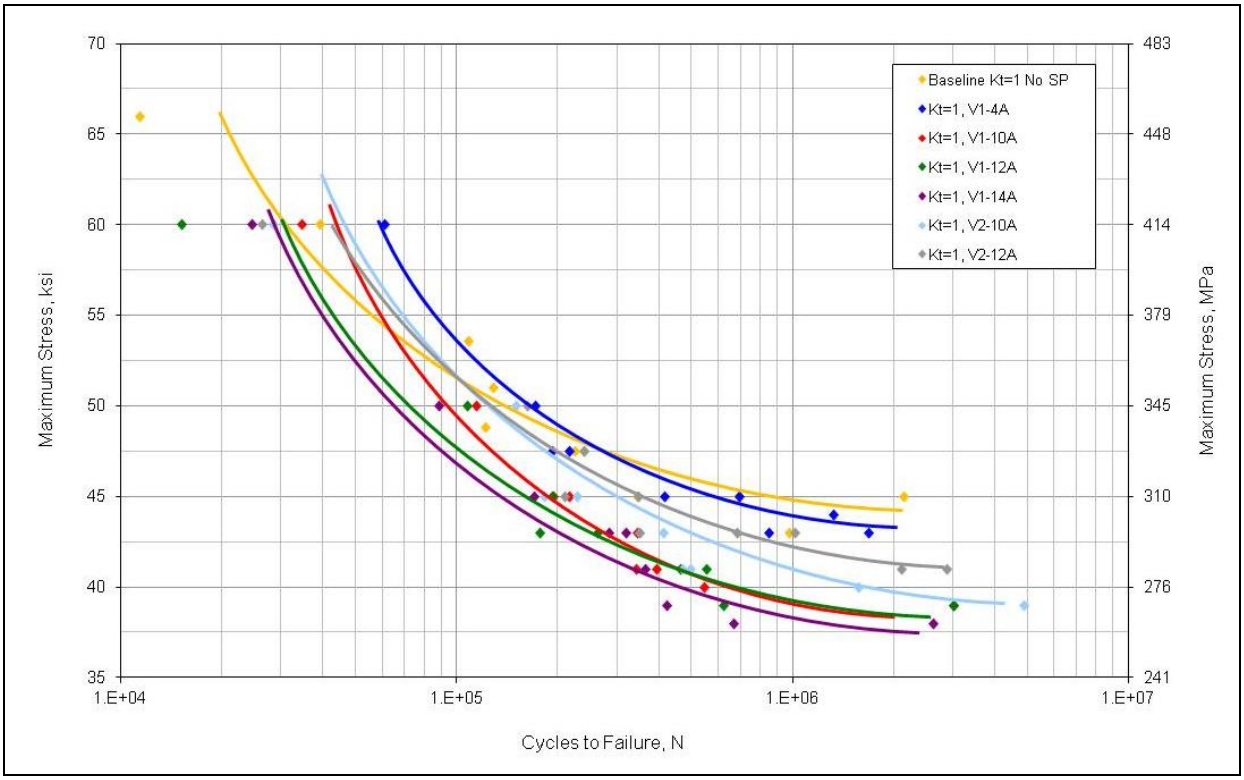

Figure 9. Fatigue data from the aluminum 7075-T73.

4. Summary

Table 4 lists the relative rankings of analytical elements from residual stress measurement and fatigue testing for each material and shot-peening condition. X-ray diffraction data were evaluated in relation to induced residual compressive stress and corresponding peak width. Fatigue performance was rated in terms of endurance limit by comparing the results from the shot-peened specimens with an identical unpeened baseline group.

Table 4. Relative rankings of analytical elements from residual stress measurement and fatigue testing.

	4340 Steel					**Carburized 9310 Steel**					**Beta STOA Titanium 6Al-4V**				**7075-T73 Aluminum**					
Vendor: Intensity:	V1 4A	V2 4A	V1 8A	V2 8A	V2 12A	V1 4A	V2 4A	V1 8A	V2 8A	V2 12A	V1 4A	V1 8A	V1 11.5A	V2 12A	V1 4A	V1 10A	V2 10A	V1 12A	V2 12A	V1 14A
Highest surface compressive stress	—	X	—	—	—	—	X	—	—	—	—	X	—		X	—	—	—	—	—
Lowest surface compressive stress	—	—	—	—	X	—	—	—	—	X	—	—	—	X	—	—	—	—	—	X
Highest subsurface compressive stress	—	—	—	X	—	—	X	—	—	—	—	X	—	—	—	—	X	—	—	—
Deepest levels of compression	—	—	—	—	X	—	—	—	—	X	—	—	X	—	—	—	—	—	—	X
Broadest x-ray diffraction peak	—	—	—	—	X	—	—	—	—	X	—	—	—	X	—	—	—	—	—	X
Narrowest x-ray diffraction peak	X	—	—	—	—	X	—	—	—	—	X	—	—	—	X	—	—	—	—	—
Best fatigue performance	—	X	—	—	—	—	X	—	—	—	X	—	—	—	X	—	—	—	—	—
Poorest fatigue performance	—	—	—	—	X	—	—	—	—	X	—	—	—	X	—	—	—	—	X	—

5. Conclusions

5.1 Residual Stress and Diffraction Peak Width Data

1. The magnitude of the residual stresses measured on the disk specimens at the center and at a radial outward (edge) location were statistically equivalent.
2. The 4340 and carburized 9310 steel profiles were similar in trend, but the 9310 stresses were more compressive.
3. The titanium and aluminum stress distributions were unique and predictably different from the steel.

4. For all materials, the broadest x-ray diffraction peak was associated with the lowest surface compressive residual stress and, in general, produced by the highest peening intensity.

5. In general, the deepest levels of compression resulted from the higher peening intensities (11.5A, 12A, and 14A).

6. Of the four materials investigated, only the aluminum remained in compression through the deepest electropolished layer, 0.254 mm (0.010 in).

5.2 Fatigue Performance

1. Uniformly, an inverse relationship was observed between shot-peening intensity and fatigue performance.

2. When compared with the unpeened baseline group, the lower shot-peening intensities proved beneficial to fatigue performance, while, in some instances, higher intensities were found to be detrimental.

3. The aluminum data demonstrated that shot peening, performed to the herein specified Almen A-scale intensities, did not improve fatigue performance.

4. The best fatigue performance correlated with the lowest shot-peening intensity, 4A, for all materials.

5. There appeared to be no significant difference between the V1 and V2 shot-peened specimens, where direct comparisons could be made. In some cases, the groups performed equally, while, in other cases, one of the vendors performed somewhat better.

Conventional thought with regard to shot-peen-induced residual compressive stresses has often been that higher magnitudes at deeper levels are preferred. This investigation showed a direct correlation of shot-peen intensity with the amount of resulting plastic deformation, as would be expected. However, for the aviation materials and the processing conditions examined, it appeared that the lower shot-peening intensities imparted a combination of residual compressive stresses and strains that were more fatigue-resistant than the higher intensities. The data also suggested that it was quite possible that common higher shot-peening intensities might be damaging from the standpoint of endurance limit fatigue performance.

X-ray diffraction was used to nondestructively measure elastic strain (residual stress) in shot-peened aviation materials. Plastic strain was evaluated by the width of the diffraction peak. Coupling elastic and plastic strain data provided a means to better assess the effectiveness of the shot-peening process and offered information for determining the optimum conditions to increase resistance to fatigue failure in either a surface-related or a damage-tolerant application.

6. References

1. AMS-S-13165. *Shot Peening of Metal Parts* **1997**.
2. Metal Improvement Co. *Shot Peening Applications Guide*; 9th ed.; Paramus, NJ, 2004.
3. Wohlfahrt, W. Shot Peening and Residual Stresses. *Proceedings of the 28th Sagamore Army Materials Research Conference*, 1982; pp 71–92.
4. Meister, J. Improving Fatigue Life of Components by Shot Peening. *Industrial Heating* **1997**; pp 57–61.
5. SAE International. *Residual Stress Measurement by X-Ray Diffraction*; SAE-J784a; 2003.
6. Noyan, I. C.; Cohen, J. B. *Residual Stress: Measurement by Diffraction and Interpretation*, Springer-Verlag: New York, 1987.
7. Cullity, B. D.; Stock, S. R. *Elements of X-Ray Diffraction*; 3rd ed.; Prentice Hall: New York, 2001.
8. Taira, S.; Kamachi, K. Detection of Fatigue Damage by X-rays. *Proceedings of the 23rd Sagamore Army Materials Research Conference*, 1979; pp 21–54.
9. AISI/SAE E4340. *Steel, Chrome-Nickel-Molybdenum Bars and Reforging Stock* **1999**.
10. AMS 2759/1C. *Heat Treatment of Carbon and Low-Alloy Steel Parts Minimum Tensile Strength Below 220 ksi (1517 MPa)* **2000**.
11. AMS 4928Q. *Titanium Alloy Bars, Wire, Forgings, and Rings* **2001**.
12. AMS-QQ-A 225/9. *Aluminum Alloy 7075, Bar, Wire, and Special Shapes; Rolled, Drawn, or Cold Finished* **1997**.
13. Grendahl, S.; Snoha, D.; Hardisky, B. *Shot-Peening Sensitivity of Aerospace Materials*; ARL-TR-4095; U.S. Army Research Laboratory: Aberdeen Proving Ground, MD, May 2007.
14. Gariby, R. P.; Chang, N. S. Improved Fatigue Life of a Carburized Gear by Shot Peening Parameter Optimization. *Proceedings of an International Conference on Carburizing: Processing and Performance*, 1989; pp 283–289.

List of Symbols, Abbreviations, and Acronyms

FWHM	full width-half maximum
HRC	hardness Rockwell “C”
RS	residual stress
STOA	solution treated and overaged
XRD	x-ray diffraction

NO. OF COPIES	ORGANIZATION
1 (PDF only)	DEFENSE TECHNICAL INFORMATION CTR DTIC OCA 8725 JOHN J KINGMAN RD STE 0944 FORT BELVOIR VA 22060-6218
1	DIRECTOR US ARMY RESEARCH LAB IMNE ALC HRR 2800 POWDER MILL RD ADELPHI MD 20783-1197
1	DIRECTOR US ARMY RESEARCH LAB RDRL CIO LL 2800 POWDER MILL RD ADELPHI MD 20783-1197

NO. OF
COPIES ORGANIZATION

1 BENET WEAPONS LAB
RDAR WSB
M MILLER
WATERVLIET ARSENAL
WATERVLIET NY 12189-4050

1 US ARMY ARDEC
RDAR MEE M
S LUCKOWSKI
BLDG 3150
PICATINNY ARSENAL NJ
07806-5000

1 US AIR FORCE RSRCH LAB
AFRL/MLLMN
M SHEPARD
2230 TENTH ST
WPAFB OH 45433-7817

5 US ARMY RDECOM
RDMR AEF M
J GRAN
D GRONER
M KANE
G LIU
R MCFARLAND
BLDG 4488 RM 211
REDSTONE ARSENAL AL 35898

1 US ARMY RDECOM
RDMR AEP M
G SAHRMANN
BLDG 4488 RM 211
REDSTONE ARSENAL AL 35898

1 US ARMY RDECOM
RDMR WDP A
A INGRAM
BLDG 7631
REDSTONE ARSENAL AL 35898

1 US ARMY RSRCH OFC
S MATHAUDHU
BLDG 12211
RESEARCH TRIANGLE PARK
NC 27709-2211

NO. OF
COPIES ORGANIZATION

ABERDEEN PROVING GROUND

1 ABERDEEN TEST CENTER
TEDT AT FP
B HARDISKY
BLDG 400
APG MD 21005

25 DIR USARL
RDRL LOA L
M ADAMSON
RDRL WM
J MCCAULEY
RDRL WML G
W DRYSDALE
RDRL WMM
J BEATTY
R DOWDING
RDRL WMM B
B CHEESEMAN
RDRL WMM D
R CARTER
K CHO
M PEPI
RDRL WMM E
J SWAB
RDRL WMM F
S GRENDAHL (2 CPS)
B BUTLER
F KELLOGG
D SNOHA (2 CPS)
L KECSKES
E KLIER
W DEROSSET
J MONTGOMERY
RDRL WMM G
F BEYER
RDRL SLB W
C KENNEDY
RDRL VT
S WILKERSON
RDRL VTM
V WEISS
RDRL VTP
B DYKAS

INTENTIONALLY LEFT BLANK.